



## Effects of five tissue sources of silver carp by-products on the structure, physicochemical and emulsifying properties of gelatin

Guangyi Kan<sup>a,b</sup>, Li Li<sup>a,b</sup>, Huan Gong<sup>a,b</sup>, Lijia Chen<sup>a,b</sup>, Xichang Wang<sup>b</sup>, Jian Zhong<sup>a,b,c,d,\*</sup>

<sup>a</sup> Medical Food Laboratory, Shanghai Key Laboratory of Pediatric Gastroenterology and Nutrition, Shanghai Institute for Pediatric Research, Xinhua Hospital, Shanghai Jiao Tong University School of Medicine, Shanghai, 200092, China

<sup>b</sup> National R&D Branch Center for Freshwater Aquatic Products Processing Technology (Shanghai), Integrated Scientific Research Base on Comprehensive Utilization Technology for By-Products of Aquatic Product Processing of Ministry of Agriculture and Rural Affairs of the People's Republic of China, Shanghai Engineering Research Center of Aquatic-Product Processing and Preservation, College of Food Science & Technology, Shanghai Ocean University, Shanghai, 201306, China

<sup>c</sup> Department of Clinical Nutrition, College of Health Science and Technology, Shanghai Jiao Tong University School of Medicine, Shanghai, 200135, China

<sup>d</sup> Marine Biomedical Science and Technology Innovation Platform of Lingang Special Area, Shanghai, 201306, China

### ARTICLE INFO

Handling Editor: Dr. Quancai Sun

#### Keywords:

Fish oil  
Gel strength  
*Hypophthalmichthys molitrix*  
Interfacial tension  
Viscosity

### ABSTRACT

The effects of tissue sources on gelatin's physicochemical and functional properties remain unclear. This work aimed to analyze the effects of five tissue sources on the properties of fish gelatins. Five gelatins were extracted from different silver carp by-products (skin, scale, fin, head, and bone) and the effects of tissue sources on the gelatin's properties were studied. The gelatin's  $\beta$ -sheet percentages and total sodium dodecyl sulfate-polyacrylamide gel electrophoresis band intensities ( $\beta$ ,  $\alpha 1$ , and  $\alpha 2$  chains) showed similar dependence to the tissue sources: skin  $\approx$  scale  $>$  fin  $\approx$  head  $>$  bone. Bone-related gelatins (from head and bone) showed lower water-holding capacity and fat-binding capacity values than the other gelatins. Tissue sources significantly affected the gelatin's gel strength values: skin  $\approx$  fin  $>$  scale  $>$  bone  $\approx$  head. Scale and bone gelatin solutions had significantly lower rheological apparent viscosities than other by-product gelatin solutions. The interfacial tension and rheological apparent viscosity values of the fish oil-loaded gelatin-stabilized emulsions depended on the gelatin tissue sources and gelatin concentrations. In particular, skin, scale, and fin gelatins induced no obvious emulsion creaming at the gelatin concentration of 10 g/L during the emulsion storage. Bone-related gelatins induced higher emulsion creaming index values for the emulsions with 10 g/L of gelatins during the emulsion storage. This work confirmed tissue sources could significantly affect the properties of gelatins. Five tissue sources had different effects on the structural, physicochemical, and emulsifying properties of silver carp by-product gelatins. Especially, the gelatins from different silver carp by-products showed different water-holding and fat-binding capacities, gel strengths, interfacial tension, rheological apparent viscosities, and emulsion stabilization abilities. These properties are important considerations for the application of silver carp by-product gelatins in food and other industries.

### 1. Introduction

Gelatins have been widely explored as emulsifiers to stabilize fish oil-in-water emulsions (Zhang et al., 2020; Chen et al., 2024). Fish oils are enriched with omega-3 polyunsaturated fatty acids and have many physiological and therapeutic functions (Du et al., 2022). The application of fish oil emulsions can encapsulate fish oil for protection, convert fish oil into water-soluble systems, and isolate the fishy taste of fish oil

(Ding et al., 2019). Until now, both mammalian and fish gelatins have been applied as emulsifiers to stabilize fish oil emulsions (Xu et al., 2021; Zhang et al., 2020).

Fish gelatin has attracted much attention among the gelatins from different animals. Fish gelatin is a partial hydrolysis polymer from native collagen in collagen-enriched sources of many fish species. It has already been considered as a promising alternative to mammalian gelatin. It was due to the several significant advantages of fish gelatin

\* Corresponding author. Shanghai Key Laboratory of Pediatric Gastroenterology and Nutrition, Shanghai Institute for Pediatric Research, Xinhua Hospital, Shanghai Jiao Tong University School of Medicine, Shanghai, 200092, China.

E-mail address: [jzhong@shsmu.edu.cn](mailto:jzhong@shsmu.edu.cn) (J. Zhong).

<https://doi.org/10.1016/j.crfs.2024.100894>

Received 26 August 2024; Received in revised form 4 October 2024; Accepted 23 October 2024

Available online 24 October 2024

2665-9271/© 2024 The Authors. Published by Elsevier B.V. This is an open access article under the CC BY-NC-ND license (<http://creativecommons.org/licenses/by-nc-nd/4.0/>).

such as low human-animal infectious risks and acceptance for some religious people (e.g., Jews, Hindus, and Muslims) compared with mammalian gelatins (Lv et al., 2019; Le and Yang, 2022; Nie et al., 2022). In the field of food science, it has been widely explored as additives (Feng et al., 2017), emulsifiers (Ding et al., 2020b), packaging materials (Chen et al., 2022), etc.

The effect of the extraction factors on the properties of fish gelatin is an important issue for the development and application of fish gelatin. Fish species (e.g., two freshwater and two marine fishes) could affect the physicochemical and functional properties of gelatins (Yang et al., 2022a). Extraction methods (e.g., acetic acid-, hot water-, and enzyme-pretreated methods) also could affect the properties of gelatins from tilapia skin (Zhang et al., 2020), tilapia fish scales (Peng et al., 2022), silver carp scale (Xu et al., 2021), and silver carp fin (Yang et al., 2022b). In addition, the enzyme amounts in the extraction process could affect the properties of gelatin from silver carp bone (Wu et al., 2022). However, the effects of tissue sources on the physicochemical and functional properties of fish gelatins have not been systematically and comprehensively explored until now.

Silver carp (*Hypophthalmichthys molitrix*) by-products are good tissue sources for the extraction of gelatins. Silver carp is one of the most widely cultured and traded fish species in the world (Jawdhari et al., 2022). It is a good fish source for surimi production and is widely used for surimi-based food production in China (Wang et al., 2023). After surimi production, fish by-products (e.g., skin, scale, fin, bone, and head; 60–70% of fish weight) are usually discarded as wastes, which might cause potential environmental issues (Zhang et al., 2020). Some silver carp by-products could be processed into value-added ingredients for novel food development. Typical ingredients include scale gelatin emulsifiers (Xu et al., 2021) and fish frames/heads hydrolysates nitrogen source (Zhang et al., 2023). Therefore, high value-added utilization of silver carp by-products is an important aquatic industry requirement.

Herein, the effects of five tissue sources of silver carp by-products on the structural, physicochemical, and emulsifying properties of gelatins were studied to analyze how their structures affect their function. The structure and function of biomolecules remain one of the major challenges in biology. First, an acetic acid-pretreated method was used to extract five silver carp by-product gelatins: skin gelatin (SKG), scale gelatin (SCG), fin gelatin (FIG), head gelatin (HEG), and bone gelatin (BOG). Second, the structural properties of the gelatins were studied. Third, the physicochemical properties of the gelatins were discussed. Fourth, the formation and stability of the fish oil emulsions stabilized by the gelatins were investigated. Finally, the emulsion-related parameters of the gelatins were studied. The results would provide useful information to understand the relationships among tissue sources, structural characteristics, physicochemical properties, and emulsifying properties of silver carp by-product gelatins. In addition, it also could guide the application of fish by-product gelatins in food and other industries.

## 2. Materials and methods

### 2.1. Materials

Frozen silver carp by-products (skins with scales, fins, heads, or bones) were bought from Hubei Boao Food Co. Ltd. (Danjiangkou City, Hubei Province, China). The skins with scales were separated to obtain skins and scales. All the by-products were washed, subpackaged in polyethylene sealing bags, and stored at  $-20^{\circ}\text{C}$  in a refrigerator. Fish oil with a DHA + EPA mass ratio of  $\geq 70\%$  (Xi'an Qianyecao Biological Technology Co., Ltd., Xi'an City, Shaanxi Province, China) was stored at  $4^{\circ}\text{C}$  in a refrigerator.

### 2.2. Gelatin extraction from silver carp by-products

Five fish gelatins were extracted from silver carp by-products using an acetic acid-pretreated method (Xu et al., 2021; Peng et al., 2022;

Yang et al., 2022a). The extraction process is shown in Fig. 1. The extraction process was conducted with a by-product: liquid ratio of 1:10 (w/v) and continuous stirring (Speed indicated in parentheses) using a magnetic stirrer. The fish skins and fins were cut into small pieces. The muscles, eyes, gills, and other contents of the fish head were removed. Then the fish head was washed and cut into small pieces (cartilage, hard bones, and skins). The spine bones were obtained by removing muscles and spikes. The spine bones were cut into vertebrae pieces. All the tissue pieces were cleaned with water. Then, fish by-products were mixed (300 rpm) with 0.1 mol/L of NaOH for 1 h to remove fats and non-collagenous proteins. After rinsing with water to pH 7, the scale, fin, head, and bone samples were mixed (300 rpm) with 0.2 mol/L ethylene diamine tetraacetic acid (Beijing Suolaibao Technology Co., Ltd., China) solution for 2 h to remove minerals. After rinsing with water to pH 7, the samples were pretreated (200 rpm, no magnetic stirring for fish skin sample) with 0.05 mol/L of acetic acid solution for 3 h. After rinsing with water to pH 7, the samples were mixed with water. The samples were heated (120 rpm) with water at  $55^{\circ}\text{C}$  for 6 h to extract the gelatins into the water. Then, the solutions were filtered with four layers of gauze and centrifuged at a speed of  $10000\times g$  for 10 min. The obtained solutions were freeze-dried to obtain solid silver carp by-product gelation samples. The gelatin production yield (Y) was obtained by dividing the obtained gelatin mass by the used silver carp by-product mass and multiplying by 100.

### 2.3. Attenuated total reflectance Fourier transform infrared spectrometry

The attenuated total reflectance Fourier transform infrared (ATR-FTIR) spectrometer (Spotlight 400, PerkinElmer, Waltham, Massachusetts, USA) was used to analyze the absorbance spectra of the obtained silver carp by-product gelatins with 16 scans. The resolution was  $1\text{ cm}^{-1}$ . SeaSolve PeakFit software (v4.12, San Jose, USA) was used for the secondary structure percentages analyses by fitting the amide I band (Xu et al., 2021).

### 2.4. Sodium dodecyl sulfate-polyacrylamide gel electrophoresis

Gelatin solution (2 g/L, pH 7.0) was mixed with  $5\times$  sodium dodecyl sulfate-polyacrylamide gel electrophoresis (SDS-PAGE) sample loading buffer (GenScript, Nanjing, China) (Zhang et al., 2020). After boiling, 10  $\mu\text{L}$  of the mixture was put in SurePAGE Bis-Tris 4–20% gel (GenScript). Protein Standard (GenScript) was also loaded into the SurePAGE gel. The electrophoresis was achieved at 120 V for 80 min in a mini-slab AE-6500 electrophoresis system (ATTO Corporation, Tokyo, Japan). After staining by a Coomassie Blue Staining Solution (Labgic Technology Co. Ltd., Beijing, China) for 3 h, the gel was destained by an aqueous mixture of ethanol/acetic acid/water (2:1:7, v/v/v) for 8 h. The gel was photographed using a digital camera.

### 2.5. Scanning electron microscopy

The freeze-dried silver carp by-product gelatins were observed using a S-3400 scanning electron microscope (SEM, Hitachi, Tokyo, Japan) (Yang et al., 2022b). The samples were prepared by attaching them to a conductive adhesive and then sputtering platinum for 50 s before SEM observation. The acceleration voltage was 5.00 kV.

### 2.6. Atomic force microscopy

Silver carp by-product gelatin solutions (2.5 g/L) were obtained by dissolving them in ultrapure water. Subsequently, 10  $\mu\text{L}$  of the samples were put on the mica surfaces and dried overnight. A Bioscope Resolve atomic force microscope (AFM, Bruker Corporation, Signal Hill, CA, USA) with the ScanAsyst in Air mode was applied to observe the morphologies of the samples (Shi et al., 2019). The scanning rate was 1.0 Hz. The spring constant of the SNL-series silicon cantilevers was 0.35 N/m.



Fig. 1. Extraction process of silver carp by-product gelatins from different tissue sources (skin, scale, fin, head, and bone).

Some tissue sources were shown on the black backgrounds. The extraction processes were performed in the glass beakers. During the extraction process, some samples were put on the plastic Petri dishes to show the sample statuses. The obtained filtered solutions were put into the plastic Petri dishes and freeze-dried to obtain the dried gelatins. Some gelatins were put in the glass vials to show the sample statuses.

The obtained images were treated with a “flatten” function in the commercial software before the subsequent analyses.

## 2.7. Gelatin gel strength

Briefly, 0.667 g of gelatin samples were dissolved in 10 mL of water in glass beakers with 25 mL specification at 45 °C for 2 h. The pH was 5.0–7.0 for these samples. The height and diameter of cylindrical gelatin gels were 12 and 33 mm, respectively. After cooling at 10 °C for 16 h, a TA. GEL Texture Analyzer (Shanghai Bosin Industrial Development Co., Ltd., Shanghai, China) with a plunger with a diameter of 1.27 cm was used to analyze the samples. The load cell specification was 50 N. The depression experiments were done for 4 mm with a plunger speed of 1 mm/s. The penetration distance was 33% of the gel height. The gel strength values (maximum forces) were recorded in N (Zhang et al., 2020).

## 2.8. Turbidity

Silver carp by-product gelatin solutions (10 g/L) were obtained by dissolving them in ultrapure water (45 °C, 180 rpm, 60 min). Then, the pH was adjusted to the designated values (3.0, 4.0, 5.0, 6.0, 7.0, 8.0, 9.0, 10.0, and 11.0) using 1 mol/L HCl solution or 1 mol/L NaOH solution. The samples were photographed using a digital camera. The transparency values of the sample solutions were measured using a T6 UV spectrophotometer (Purkinje General Instrument Co. Ltd., Beijing, China) at 600 nm and the transparency values were (Zhang et al., 2020).

## 2.9. Rheological measurements

Silver carp by-product gelatin solutions (50 g/L) were obtained by dissolving them in ultrapure water (45 °C, 180 rpm, 60 min). The gelatin solution pH was adjusted to 7.0. Silver carp by-product gelatin solutions (2, 6, and 10 g/L, pH 7.0) were mixed with fish oil (1:1, v/v). The

mixtures were homogenized at 11500 rpm for 60 s to obtain emulsions using a T 10 basic ULTRA-TURRAX® homogenizer (10 mm head, IKA, Guangzhou, China) (Ding et al., 2020b).

The rheological properties of the gelatin solutions and emulsions were examined using a DHR-3 Discovery Hybrid Rheometer (TA Instruments, Inc., New Castle, DE, USA) with a parallel plate (diameter: 40 mm) at 25 °C (Primožic et al., 2017; Netter et al., 2020). The operating gap was 1 mm. Strain sweeps were performed at the shear strain range of 0.1%–100% and the constant frequency of 1 rad/s. The viscosity (Pa·s) was shown at different shear rates (1/s). The storage modulus (G′) and loss modulus (G″) were shown at strain (%).

### 2.10. Water-holding capacity and fat-binding capacity

The freeze-dried gelatins (0.1 g) were added to 5 mL of water or fish oil in 20 mL glass vials. The samples were vortexed for 5 s and stood for 2 min to see the gelatin status in water or fish oil. To analyze water-holding capacity (WHC) and fat-binding capacity (FBC), the gelatins (0.1 g) were added to 5 mL of water or fish oil in 50 mL centrifuge tubes. The samples were vortexed for 5 s every 15 min in 1 h. After centrifuging (450×g) for 20 min, the top liquids were removed and the tubes were tilted (45° angle) for 30 min to let the unadsorbed fish oil flow away. The values (g/g) were obtained by dividing the differences between the remained content masses and the used gelatins by the used gelatins (Shyni et al., 2014).

### 2.11. Emulsion preparation and storage stability

Silver carp by-product gelatin solutions (2, 6, and 10 g/L, pH 7.0) were mixed with fish oil (1:1, v/v). The mixtures were homogenized at 11500 rpm for 60 s to obtain emulsions using a T 10 basic ULTRA-TURRAX® homogenizer (10 mm head, IKA, Guangzhou, China) (Ding et al., 2020b). At room temperature, the emulsions were photographed and the creaming index (CI) values were analyzed by dividing the serum height by the emulsion height and multiplying by 100.

The emulsion droplets were observed using an ML8000 upright optical microscope (Shanghai Minz Precision Instruments Co. Ltd., Shanghai, China) with an objective of 40 × . Three batches of experiments were performed and some images were randomly selected from each batch. The emulsion droplet sizes in these images were completely measured (300–800 droplets). The frequency distribution was analyzed with multiple peak Gauss fitting (Ding et al., 2020a).

### 2.12. Emulsifying parameters

Silver carp by-product gelatin solutions (C = 2, 6, and 10 g/L, pH 7.0) were used to prepare emulsions, as described in Section 2.9. At 0 and 10 min, 20 μL of the liquid emulsion was diluted (Dilution factor = 300) with 5.98 mL of SDS solution (0.001 g/mL). After vortexing for 10 s, the UV–vis absorbances (A<sub>0</sub> and A<sub>10</sub> at 0 and 10 min, respectively) of the samples were determined using the T6 UV spectrophotometer at 500 nm. The parameters were obtained (Zhang et al., 2022):

$$\text{Emulsion activity index (EAI, m}^2/\text{g)} = \frac{2 \times 2.303 \times A_0 \times 300}{0.5 \times C \times 10000} \quad (1)$$

$$\text{Emulsion stability index (ESI, min)} = \frac{A_0 \times 10}{A_0 - A_{10}} \quad (2)$$

where 2 is the equation coefficient and 2.303 is the conversion value of ln and log (Wanyi et al., 2020).

### 2.13. Interfacial tension

A PZ-A2 surface tension meter (Beijing Pinzhichuangsi Precision Co., Ltd., Beijing, China) was applied to analyze the interfacial tension between fish oil and silver carp by-product gelatin solutions (2, 6, and 10

g/L) (Gong et al., 2024b). Fish oil (10 mL) was added to the gelatin solution (10 mL) in a 25 mL glass beaker. A platinum ring was put into the fish oil. After taring the interfacial tension, the platinum ring was put in the gelatin solution for 5 min. The interfacial tension (the maximum force) was obtained in mN/m when the ring was pulled out.

### 2.14. Emulsion apparent viscosity

Silver carp by-product gelatin solutions (2, 6, and 10 g/L, pH 7.0) were used to prepare emulsions, as described in Section 2.9. The emulsion's apparent viscosity was measured using the NDJ-5S digital display rotary viscometer (Shanghai Jingtian Electronic Instrument Co., Ltd., Shanghai, China) (Liu et al., 2023). The used rotor was type 4 with a cylindrical shape (11.5 cm in length and 0.3 cm in diameter). The emulsion height was 8.4 cm and the rotor was immersed in the emulsions with a depth of 3.6 cm. The rotary speed was 60 rpm.

### 2.15. Statistical analysis

Four batches of gelatins were extracted from each tissue source. Three batches of samples were prepared for each experimental analysis. The data were described as mean ± standard deviation (n = 3). One-way ANOVA with Duncan analysis was used to analyze significant differences (p < 0.001).

## 3. Results and discussion

### 3.1. Production yields of silver carp by-product gelatins

Five types of fish gelatins (SKG, SCG, FIG, HEG, and BOG) were extracted from different silver carp by-products (skin, scale, fin, head, and bone) using a classical acetic acid-pretreated method (Fig. 1) (Xu et al., 2021; Peng et al., 2022; Yang et al., 2022a). The production yields were dependent on the tissue sources: 26.0% ± 1.3% (skin) > 17.4% ± 0.5% (scale) > 3.4% ± 0.2% (head) > 3.0% ± 0.1% (fin) > 1.4% ± 0.1% (spine bone). The production yield (26.0% ± 1.3%) of SKG was slightly higher than that (23.2% ± 1.3%) from silver carp skin in our previous work (Yang et al., 2022a). The production yield (17.4% ± 0.5%) of SCG was slightly lower than that (18.7% ± 1.4%) from the silver carp scale in our previous work (Xu et al., 2021). The production yield (3.0% ± 0.1%) of FIG was slightly lower than that (5.8% ± 0.8%) from silver carp fin in our previous work (Yang et al., 2022b). The production yield differences between this and previous works were acceptable because of their differences such as fish harvest time and extraction parameters. The increase in the acid concentration, extraction time, and extraction temperature generally can increase the extraction yields (Kołodziejaska et al., 2008; Boran and Regenstein, 2009; Gong et al., 2024). Low values of the extraction parameters might induce low extraction yields and high values of the extraction parameters might induce some impurities in the final products (Gong et al., 2024). Therefore, appropriate extraction parameters should be considered to extract gelatins.

### 3.2. Structural properties of silver carp by-product gelatins

The sources can significantly affect the molecular weights and amino acid compositions of the obtained gelatins, which further affect their molecular structures (Zhang et al., 2020). ATR-FTIR spectra of five silver carp by-product gelatins (Fig. 2A) showed five obvious bands (Amide A, Amide B, Amide I, Amide II, and Amide III), which were similar to the silver carp skin gelatin (Yang et al., 2022a), scale gelatin (Xu et al., 2021), and fin gelatin (Yang et al., 2022b). Bone-related gelatins (HEG and BOG) had higher peak heights of Amide B bands and wider peak widths of Amide II bands than other gelatins. Considering the only difference among these five gelatins was the tissue source, they might result from the differences between bone-related tissues (head and spine

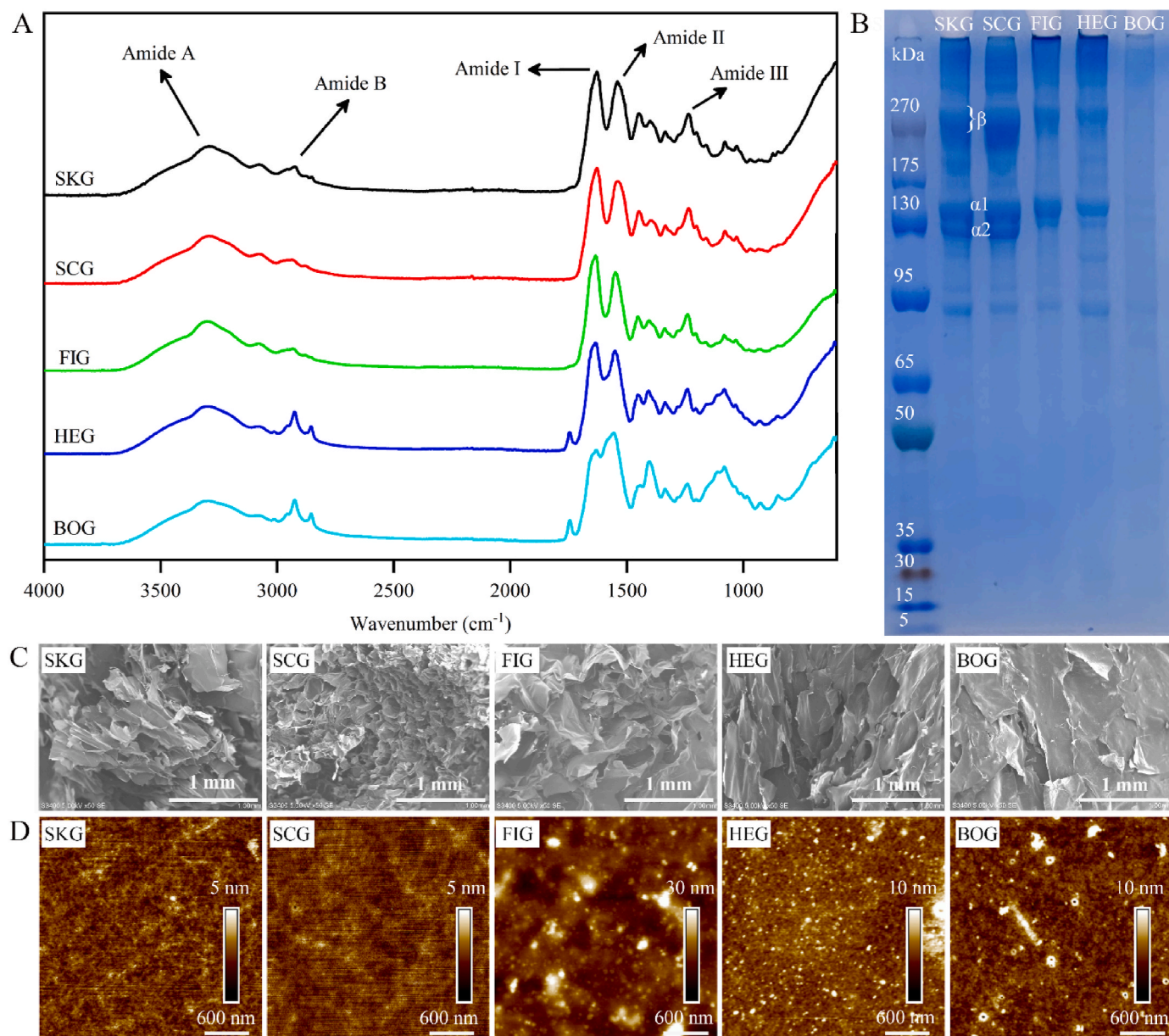


**Fig. 2.** Structural properties of silver carp by-product gelatins. (A): ATR-FTIR absorbance spectra. (B): SDS-PAGE patterns. The first lane is the protein standard (PS). (C): Scanning electron microscopy images. White scale bars indicate 1 mm. (D): Atomic force microscopy images. White scale bars (600 nm) are for XY directions. Z scales (5, 10, or 30 nm) are for Z directions.

bone) and nonbone-related tissues (skin, scale, and fin). Therefore, the bone-related gelatins (HEG and BOG) had more asymmetrical stretching of CH<sub>2</sub> (Amide B) and N-H bending coupled with CN stretching (Amide II) (Noguchi and Sugiura, 2003; Hasanuddin et al., 2024) than other gelatins (SKG, SCG, and FIG).

The secondary structure percentages were obtained by fitting the Amide I bands (1700–1600 cm<sup>-1</sup>) of ATR-FTIR spectra (Fig. S1). For all the gelatins, the secondary structure percentages order was (Table 1):  $\beta$ -sheet  $\geq$   $\beta$ -turn  $>$   $\alpha$ -helix  $\approx$  random coil  $>$   $\beta$ -antiparallel. The order was almost similar to that of silver carp fin gelatin (Yang et al., 2022b) and scale gelatin (Xu et al., 2021) in our previous works. All the gelatins showed similar  $\alpha$ -helix, random coil, and  $\beta$ -antiparallel percentages. The  $\beta$ -sheet percentages were dependent on gelatin tissue sources: SKG  $\approx$  SCG  $>$  FIG  $\approx$  HEG  $>$  BOG. The  $\beta$ -turn percentage order of the gelatins was reversely consistent with the  $\beta$ -sheet percentage.

The molecular weight distribution of silver carp by-product gelatins was examined using the SDS-PAGE technique (Fig. 2B). BOG showed no

**Table 1**

Secondary structure percentage (%) of silver carp by-product gelatins by analyzing the areas of 1600–1700 cm<sup>-1</sup> in ATR-FTIR. Different letters indicate significant differences ( $p < 0.001$ ) in each column.

| Type of gelatin | $\beta$ -sheet (%)            | random coil (%)               | $\alpha$ -helix (%)           | $\beta$ -turn (%)              | $\beta$ -antiparallel (%)    |
|-----------------|-------------------------------|-------------------------------|-------------------------------|--------------------------------|------------------------------|
| SKG             | 45.80 $\pm$ 0.95 <sup>a</sup> | 14.37 $\pm$ 0.57 <sup>f</sup> | 13.41 $\pm$ 0.30 <sup>f</sup> | 22.25 $\pm$ 0.78 <sup>e</sup>  | 4.17 $\pm$ 0.48 <sup>g</sup> |
| SCG             | 45.17 $\pm$ 0.78 <sup>a</sup> | 13.93 $\pm$ 0.48 <sup>f</sup> | 13.03 $\pm$ 0.27 <sup>f</sup> | 23.29 $\pm$ 1.07 <sup>de</sup> | 4.57 $\pm$ 0.47 <sup>g</sup> |
| FIG             | 40.43 $\pm$ 0.99 <sup>b</sup> | 15.02 $\pm$ 0.19 <sup>f</sup> | 14.77 $\pm$ 0.17 <sup>f</sup> | 25.44 $\pm$ 0.49 <sup>d</sup>  | 4.34 $\pm$ 0.14 <sup>g</sup> |
| HEG             | 41.86 $\pm$ 0.81 <sup>b</sup> | 14.72 $\pm$ 0.47 <sup>f</sup> | 14.35 $\pm$ 0.09 <sup>f</sup> | 24.91 $\pm$ 1.08 <sup>de</sup> | 4.15 $\pm$ 0.11 <sup>g</sup> |
| BOG             | 32.79 $\pm$ 2.08 <sup>c</sup> | 14.80 $\pm$ 0.06 <sup>f</sup> | 15.97 $\pm$ 0.23 <sup>f</sup> | 32.10 $\pm$ 1.61 <sup>c</sup>  | 4.34 $\pm$ 0.28 <sup>g</sup> |

obvious protein bands, which was consistent with the silver carp spine bone gelatin using pepsin enzyme method (Wu et al., 2022). In addition, grass carp skin gelatin using a trypsin pretreatment method also showed low molecular weights from 15 to 25 kDa (Ruan et al., 2023). It suggested that the collagens in the silver carp spine bones could be easily hydrolyzed into protein molecules with small molecular weights of <5 kDa. All other four gelatins showed the  $\beta$  chain (SKG and SCG: 260 kDa. FIG and HEG: 280 kDa),  $\alpha 1$  chain (SKG and SCG: 140 kDa. FIG and HEG: 150 kDa), and  $\alpha 2$  chain (SKG and SCG: 120 kDa. FIG and HEG: 130 kDa) of collagen. The SDS-PAGE patterns of SKG, SCG, and FIG were similar to the silver carp fin gelatin (Yang et al., 2022b), scale gelatin (Xu et al., 2021), and skin gelatin (Yang et al., 2022a) in our previous work. The other four gelatins showed similar molecular weight patterns with slightly different gelatin molecular weights (SKG  $\approx$  SCG < FIG  $\approx$  HEG). The total SDS-PAGE band intensities of  $\beta$ ,  $\alpha 1$ , and  $\alpha 2$  chains were dependent on the tissue sources: SKG  $\approx$  SCG > FIG  $\approx$  HEG > BOG. The order was consistent with the  $\beta$ -sheet percentage order (Table 1) and reversely consistent with the  $\beta$ -turn percentage order (Table 1). Previous work suggested that the gelatin molecular weight distribution and intensity were dependent on fish sources and extraction methods (Peng et al., 2022; Yang et al., 2022a; Yu et al., 2023). This work further suggested that the gelatin molecular weight distribution and intensity were also dependent on tissue sources. Therefore, fish sources, tissue sources, and extraction methods are important factors for the extraction and application of fish gelatins.

In the SEM images (Fig. 2C), the freeze-dried silver carp by-product gelatins showed sheet-like structures, which were similar to silver carp fin gelatin (Yang et al., 2022b), silver carp scale gelatin (Xu et al., 2021), and silver carp skin gelatin (Yang et al., 2022a). The sheet sizes were dependent on the gelatin tissue sources: SCG  $\approx$  SKG < FIG  $\approx$  HEG < BOG. The order was reversely consistent with the  $\beta$ -sheet percentage order (Table 1) based on the ATR-FTIR results and the total SDS-PAGE band intensities of  $\beta$ ,  $\alpha 1$ , and  $\alpha 2$  chains in the SDS-PAGE pattern (Fig. 2B). The order was consistent with the  $\beta$ -turn percentage order (Table 1) based on the ATR-FTIR results. Therefore, the morphologies of the freeze-dried gelatin samples were mainly dependent on the protein SDS-PAGE band intensities and secondary structure percentages ( $\beta$ -sheet and  $\beta$ -turn).

In AFM images (Fig. 2D), the dried silver carp by-product gelatin samples showed different deposited molecular aggregates. Both SKG and SCG showed nanoparticle-aggregated layers. FIG showed large nanoparticles. Both HEG and BOG showed small nanoparticles. Protein self-assembly behaviors depend on the molecular bond interaction-based supramolecular strategies (Bai et al., 2016). The aggregate sizes in the AFM results (Fig. 2D) were dependent on the tissue sources: FIG > HEG  $\approx$  BOG > SKG  $\approx$  SCG. It might partially explain the differences in the ATR-FTIR spectra (Amide B, Amide I, and Amide II) between bone-related gelatins (HEG and BOG) and other gelatins (SKG, SCG, and FIG) in Fig. 2A. However, the aggregate size order did not show an obvious relationship to the SDS-PAGE pattern (Fig. 2B). It suggested that

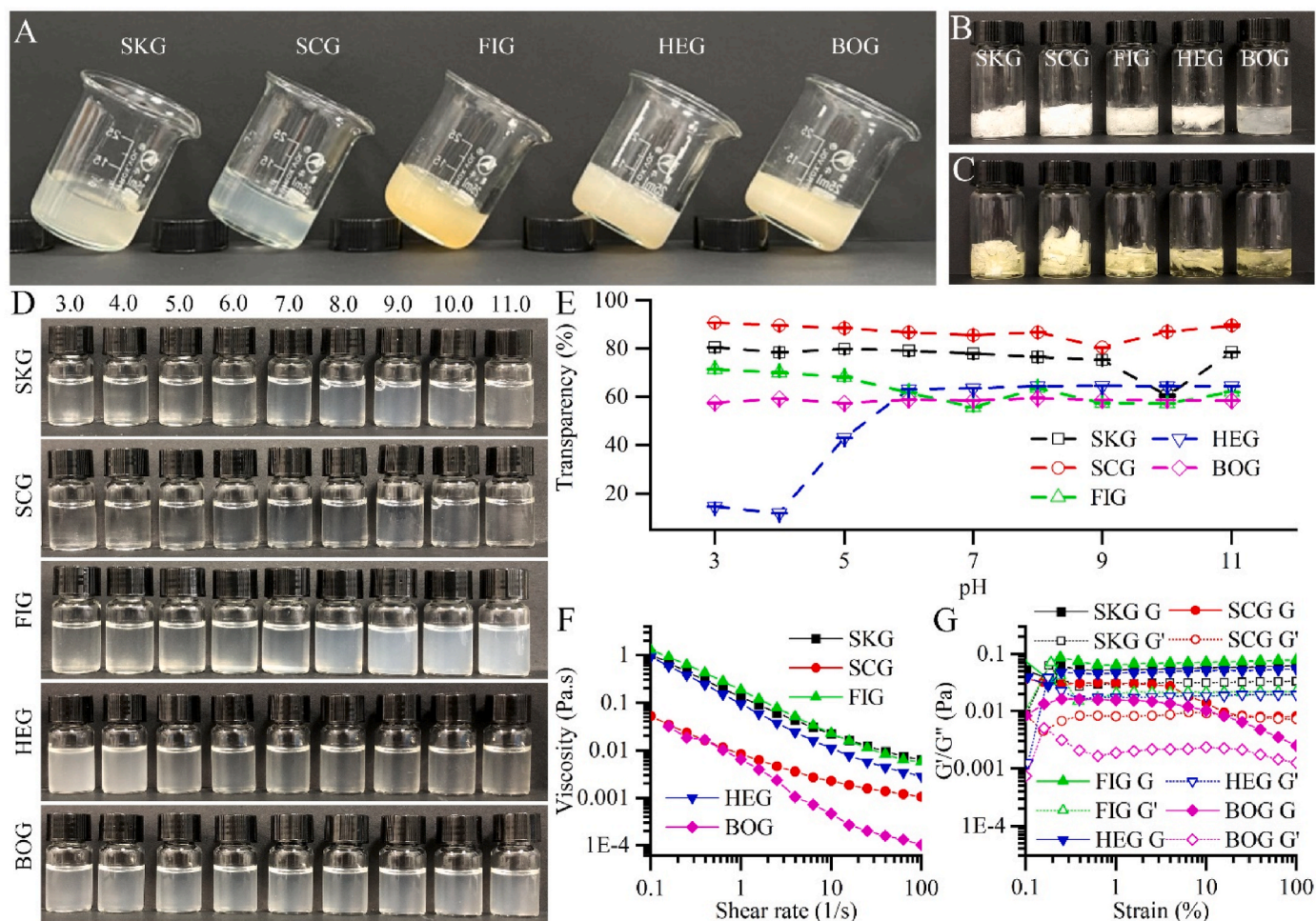


**Fig. 3.** Physicochemical properties of silver carp by-product gelatins. (A): Digital camera images of gelatin gels. (B): Digital camera images of gelatins in water. (C): Digital camera images of gelatins in fish oil. (D): Digital camera images of gelatin solutions at different pH (From left to right: 3.0–11.0). The gelatin solutions were stewed for 1 h at room temperature. (E): Transparency values of the gelatin solutions in (D). (F): Viscosity curves of the gelatin solutions. (G): Strain sweep curves of the gelatin solutions.

the aggregate behaviors of the gelatins were not related with their molecular weight distribution.

### 3.3. Physicochemical properties of silver carp by-product gelatins

All the silver carp by-product gelatins could form gels at 10 °C (Fig. 3A). A large number of gelatin mass (7.5 g of gelatin with 105 mL water) was required for the gel strength Bloom measurement of a gelatin (Yang et al., 2022a). However, the production yields of three gelatins were low (FIG: 3.0% ± 0.1%; HEG: 3.4% ± 0.2%; and BOG: 1.4% ± 0.1%). Therefore, the Bloom values of these five gelatins were not measured and the gel strength values were measured. The gel strength values of the gelatins in glass beakers (Fig. 3A) were dependent on the gelatin tissue sources (Table 2): SKG (7.18 ± 0.43 N) ≈ FIG (6.95 ± 0.42 N) > SCG (5.36 ± 0.37 N) > BOG (4.17 ± 0.20 N) ≈ HEG (4.03 ± 0.06 N). Due to the technique difference, the obtained gel strength values (Table 2) were higher than the Bloom values (Yang et al., 2022a). It was important to choose appropriate tissue sources when aquatic gelatins were considered to be used in food development. The gel strength Bloom value of silver carp skin gelatin was 361 ± 1 Bloom (Yang et al., 2022a). Therefore, the gel strength Bloom values of silver carp by-product gelatins were from 361 to 202 Bloom if the measured Bloom and g values were assumed in a multiple relationship. The by-product gelatins fit well with the high-Bloom (200–300 Bloom) gelatins (Haug and Dragnet, 2011). It suggested the silver carp by-product gelatins might be promising replacers as mammalian gelatins with high-Bloom.

The silver carp by-product gelatins were added in water (Fig. 3B) and fish oil (Fig. 3C) and then vortexed for 5 s. After 2 min, the silver carp by-product gelatins showed different solubility behaviors in the liquids. The bone-related gelatins (HEG and BOG) showed better solubility in both water and fish oil than the other gelatins. Both WHC and FBC values (Table 2) were dependent on the gelatin tissue sources. Bone-related gelatins (HEG and BOG) showed relatively lower WHC (10.0 ± 0.6–13.1 ± 0.8 g/g) and FBC (6.7 ± 0.4–6.7 ± 0.7 g/g) values than the other gelatins (WHC: 18.6 ± 0.7–37.6 ± 0.8 g/g; FBC: 15.0 ± 0.2–25.7 ± 1.1 g/g). Moreover, SKG and SCG showed a reverse order between WHC and FBC values. The results were consistent with that the sources can significantly affect the molecular weights and amino acid compositions of the obtained gelatins, which further affect their physicochemical properties (Zhang et al., 2020).

At different solution pH (3.0–11.0), all the silver carp by-product gelatins showed different turbidity behaviors (Fig. 3D). The transparency values of the gelatin solutions (Fig. 3E) showed the gelatins had different isoelectric points (pIs). The trends of SKG and SCG were consistent with silver carp skin gelatin (Yang et al., 2022a) and scale gelatin (Xu et al., 2021), respectively. SKG and SCG solutions were more transparent than other gelatin solutions and showed the basic pIs of pH 9.0 and 10.0, respectively. HEG solution was relatively turbid and showed an acidic pI of 4.0. FIG solution was significantly turbid at a pH of ≥7.0. BOG solution was significantly turbid at all the pH ranges (3.0–11.0). The differences were due to the gelatin aggregation behaviors in the solutions. It explained that FIG had the largest nanoparticles among the gelatins in the AFM images (Fig. 2D). Therefore, the five gelatin solutions showed different turbidity.

The rheological properties of silver carp by-product gelatin solutions

**Table 2**

Gel strength values of gelatin gels. Water-holding capacity. Fat-binding capacity. Different letters indicate significant differences ( $p < 0.001$ ) in each column.

| Type of gelatin | Gel strength (N)          | Water-holding capacity (g/g) | Fat-binding capacity (g/g) |
|-----------------|---------------------------|------------------------------|----------------------------|
| SKG             | 7.18 ± 0.43 <sup>a</sup>  | 37.6 ± 0.8 <sup>a</sup>      | 15.0 ± 0.2 <sup>b</sup>    |
| SCG             | 5.36 ± 0.37 <sup>b</sup>  | 26.2 ± 0.6 <sup>b</sup>      | 25.7 ± 1.1 <sup>a</sup>    |
| FIG             | 6.95 ± 0.42 <sup>a</sup>  | 18.6 ± 0.7 <sup>c</sup>      | 16.2 ± 0.4 <sup>b</sup>    |
| HEG             | 4.03 ± 0.06 <sup>c</sup>  | 10.0 ± 0.6 <sup>e</sup>      | 6.7 ± 0.7 <sup>c</sup>     |
| BOG             | 4.17 ± 0.20 <sup>bc</sup> | 13.1 ± 0.8 <sup>d</sup>      | 6.7 ± 0.4 <sup>c</sup>     |

were analyzed using a rheometer. The apparent viscosities of the gelatin solutions (Fig. 3F) decreased with the increase of the shear rate, which suggested the gelatin solutions were typical pseudoplastic fluids with a shear-thinning effect (Huang et al., 2020). The apparent viscosities were dependent on the shear rates and the gelatin sources. Moreover, SCG and BOG showed significantly lower viscosities than other by-product gelatins. The strain (Fig. 3G) sweep showed that  $G'$  values were higher than  $G''$ , which also demonstrated the solutions were in typical pseudoplastic fluid states (Chen et al., 2012; Lin et al., 2024). The  $G'$  and  $G''$  were also dependent on the gelatin sources.

### 3.4. Formation and stability of emulsions stabilized by silver carp by-product gelatins

Five types of silver carp by-product gelatins were used to prepare fish oil-loaded emulsions at different gelatin concentrations (2, 6, and 10 g/L). After the homogenization preparation, all the emulsions were milk-white (Fig. 4A: Camera images), which was consistent with our previous works on fish oil-loaded gelatin-stabilized emulsions (Xu et al., 2021; Yang et al., 2022b). The emulsions consisted of microscale droplets in the optical microscopy images (Fig. 4A: 2 g/L, 6 g/L, and 10 g/L). Moreover, the droplet sizes were trimodal (Fig. 4B–F and S2). For all the silver carp by-product gelatins, the droplet sizes decreased with the increasing gelatin concentrations, which was consistent with the behaviors of fish oil-loaded gelatin molecules or nanoparticle-stabilized emulsions at different gelatin concentrations (Ding et al., 2020b).

The droplet sizes were larger than those induced by silver carp fin gelatin (Yang et al., 2022b), scale gelatin (Xu et al., 2021), and skin gelatin (Yang et al., 2022a) in our previous works. It might result from the different homogenization pH and time. The homogenization pH in these three previous works was 9.0 and the homogenization pH in this work was 7.0. The homogenization time for the emulsions induced by silver carp scale gelatin was 90 s and the homogenization time in other works was 60 s. Previous works found that droplet sizes decreased with the increase in homogenization pH and time (Ding et al., 2019, 2020a). Therefore, it was reasonable that the droplet sizes in this work were larger than those in the three previous works. Moreover, the droplet sizes were dependent on the gelatin tissue sources and the gelatin concentrations (Fig. 4B–F and S2). Among these samples, SKG at 10 g/L showed the lowest droplet sizes (Fig. 4B) and FIG at 2 g/L showed the highest droplet sizes (Fig. 4D).

With time for 28 days (Fig. 5 and Fig. S3), the droplet sizes of all the emulsions increased with time due to droplet coalescence (Li and Van der Meeren, 2022). The emulsions stabilized by four types of gelatins (SKG, SCG, FIG, and HEG) became gels (indicated by asterisks) on day 1, which was consistent with the emulsions stabilized by silver carp scale gelatin (Xu et al., 2021). However, BOG-stabilized emulsions became gels (indicated by asterisks) at day 28, which was consistent with the emulsions stabilized by pepsin enzyme-pretreated silver carp bone gelatin (Wu et al., 2022). Therefore, the liquid-gel transition ability of silver carp by-product gelatin-stabilized emulsions was not dependent on the extraction methods but dependent on the tissue sources. The liquid-gel transition might result from the protein SDS-PAGE band intensities in the gelatin samples (Fig. 2B). BOG showed the lowest intensity, and therefore, the corresponding emulsion showed the slowest liquid-gel transition.

The emulsion creaming stability was dependent on both the tissue sources and the gelatin concentrations (Fig. 5A–E). The emulsion creaming with high-concentration gelatin was generally lower than that with low-concentration gelatin. It was consistent with that with bovine bone gelatin (Ding et al., 2020b). Moreover, the CI orders were different at different gelatin concentrations (Fig. 5F–H). SCG, SKG, and FIG at 10 g/L induced no obvious creaming. These three gelatins showed similar ATR-FTIR absorbance spectra (Fig. 2A), higher  $\beta$ -sheet percentages (Table 1), more high-molecule-weight fragments in SDS-PAGE pattern (Fig. 2B). Therefore, the CI values were mainly dependent on the

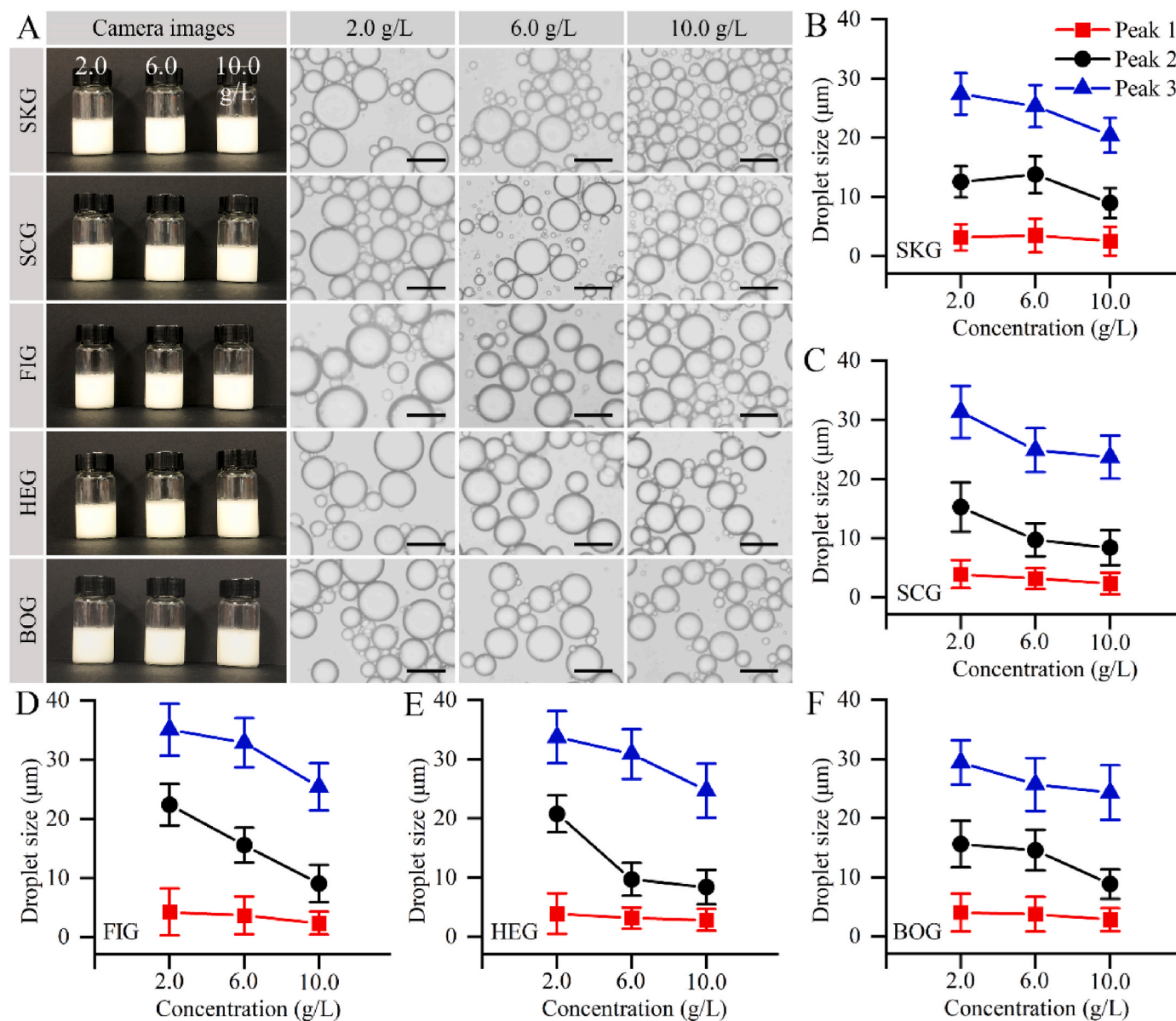


Fig. 4. Freshly prepared fish oil-loaded silver carp by-product gelatin-stabilized emulsions with different concentrations. (A): Camera images and optical microscopy images. Black scale bars indicate 40  $\mu\text{m}$ . (B–F): Dynamic droplet size spectra of the most probable sizes in the emulsions.

molecular structures and weights of the gelatins from tissue sources. The gelatins with higher  $\beta$ -sheet percentages and more high-molecule-weight fragments had better emulsion stabilization ability. SCG at 2 g/L induced the highest CI values ( $20.8\% \pm 0.8\%$ ). At the gelatin concentrations of 6 and 10 g/L (Fig. 5G and H), the bone-related gelatins (HEG and BOG) induced higher CI values than the other gelatins. Lower WHC and FBC values (Table 2) might induce lower emulsion interfacial layer thickness (Zhang et al., 2020), and therefore, induce higher CI values for the emulsions stabilized by bone-related gelatins.

### 3.5. Parameters of emulsions stabilized by silver carp by-product gelatins

The emulsifying properties of silver carp by-product gelatins were studied at different gelatin concentrations (Fig. 6A and B). The EAI decreased and ESI increased with the increasing gelatin concentrations. The behaviors were in agreement with that of the silver carp fin gelatin (Yang et al., 2022b) and tilapia scale gelatin (Peng et al., 2022) in our previous works. In addition, both EAI and ESI values were dependent on the gelatin tissue sources, and the relationships were different at

different gelatin concentrations (Fig. 6A and B). It suggested that some gelatins might show different aggregation behaviors at different concentrations, and therefore, the five gelatins showed inconsistent relationships at these concentrations. At 10 g/L of gelatin concentration, bone-related gelatins (HEG and BOG) showed higher EAI and lower ESI than the other gelatins. It explained that the bone-related gelatins induced higher emulsion CI values for the emulsions with 10 g/L of gelatins (Fig. 5H). The gelatins with lower  $\beta$ -sheet percentages (Table 1) and less high-molecule-weight fragments (Fig. 2B) induced higher EAI and lower ESI values.

The interfacial tension between silver carp by-product gelatins and fish oil showed the tension values were between  $13.4 \pm 0.1$  and  $20.2 \pm 0.2$  mN/m (Fig. 6C). Moreover, the interfacial tension values were dependent on the gelatin tissue sources and gelatin concentrations. SKG and BOG had the lowest interfacial tension values at the gelatin concentration of 6 g/L. The interfacial tension values of the other three gelatins (SCG, FIG, and HEG) decreased with the increasing gelatin concentrations, which was in agreement with the effect of gelatin nanoparticle concentrations on the interfacial tension between gelatin



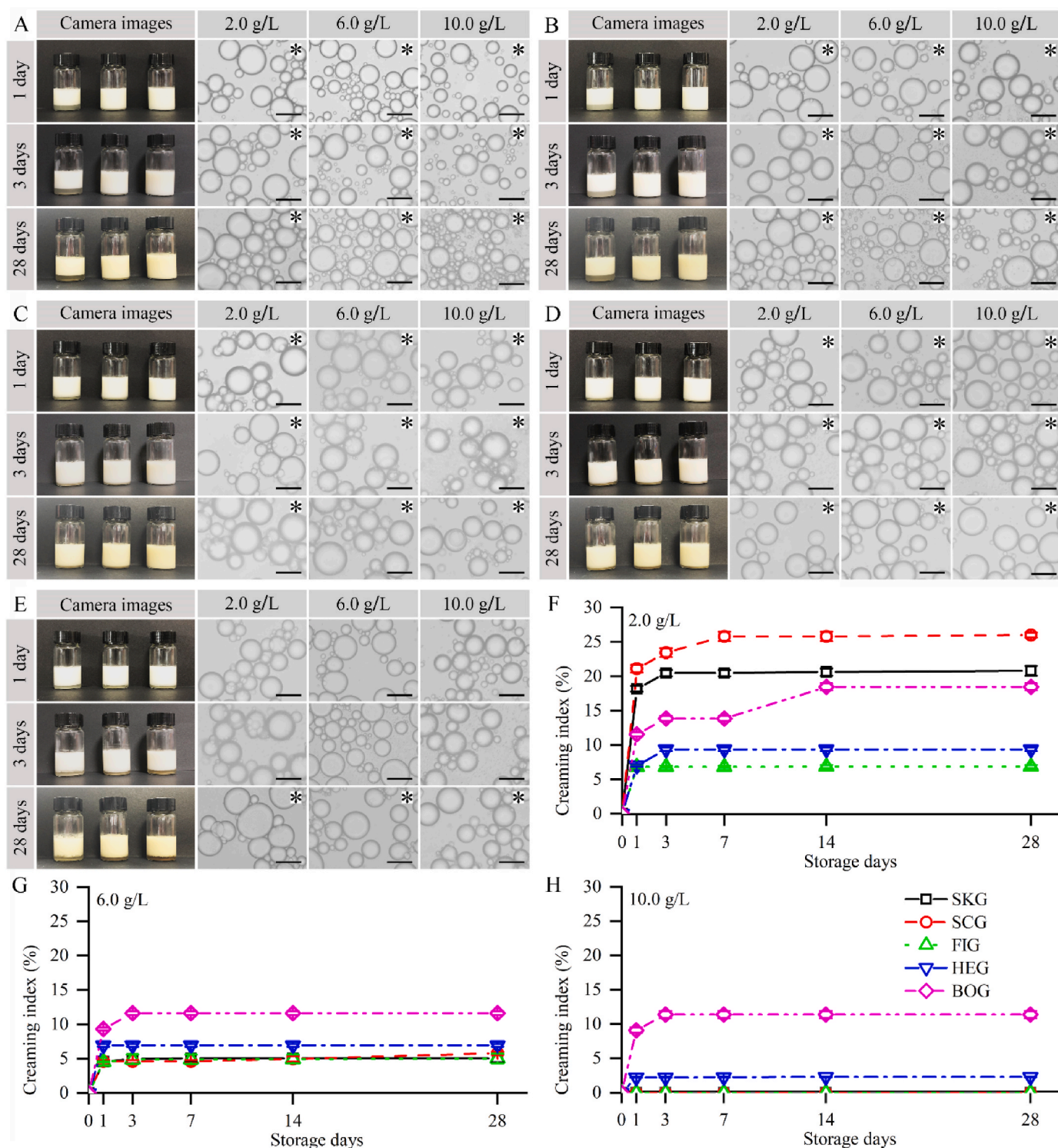


**Fig. 5.** Storage stability of fish oil-loaded emulsions stabilized by silver carp by-product gelatins at different concentrations at room temperature. (A): SKG. (B): SCG. (C): FIG. (D): HEG. (E): BOG. Asterisks indicate gels. Black scale bars indicate 40  $\mu\text{m}$ . (F): Creaming index values with a silver carp by-product gelatin concentration of 2 g/L (G): Creaming index values with a silver carp by-product gelatin concentration of 6 g/L. (F) Creaming index values with a silver carp by-product gelatin concentration of 10 g/L.

nanoparticles and fish oil (Gong et al., 2024a,b).

The emulsion apparent viscosity of fish oil-loaded silver carp by-product gelatins was between  $77.1 \pm 1.5$  and  $130.0 \pm 2.1$  mPa s (Fig. 6D). Moreover, the emulsion apparent viscosity values slightly increased with the increasing gelatin concentrations, which was in agreement with the effect of gelatin nanoparticle concentrations on the

apparent viscosity of gelatin nanoparticle-stabilized emulsions (Gong et al., 2024a,b). In addition, the apparent viscosity was also dependent on the gelatin tissue sources. BOG showed the lowest molecular weight according to the SDS-PAGE result (Fig. 2B), which might induce the lowest viscosity among these gelatins. Therefore, BOG induced the slowest liquid-gel transition (Fig. 5E). In addition, BOG induced the

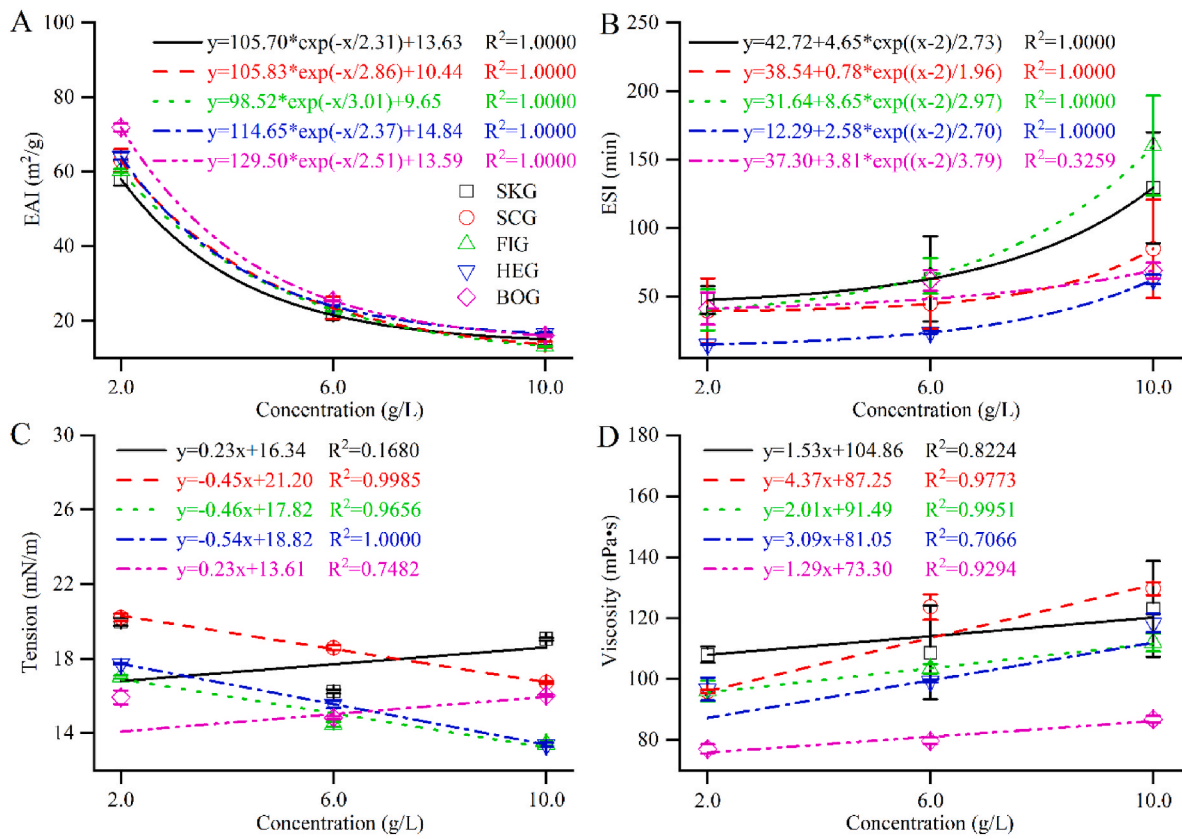


Fig. 6. Emulsion-related parameters of silver carp by-product gelatins at different gelatin concentrations at room temperature (20–24 °C). (A): Emulsion activity index (EAI). (B): Emulsion stability index (ESI). (C): Interfacial tension between gelatins and fish oil. (D): Emulsion viscosity.

highest emulsion CI values at the gelatin concentrations of 6 and 10 g/L (Fig. 5G and H) among these gelatins.

The rheological properties of the emulsions stabilized by silver carp by-product gelatins were analyzed using a rheometer. The apparent viscosities (Fig. 7A–C) decreased with the increase of the shear rate, which suggested the emulsions were typical pseudoplastic fluids with a shear-thinning effect (Huang et al., 2020). Similar to the gelatin

solutions (Fig. 3F), the emulsions also showed apparent viscosity dependence on the shear rates and the gelatin sources. Moreover, the apparent viscosities of the emulsions were also dependent on the gelatin concentrations. The strain (Fig. 7D–F) sweep showed that  $G'$  values were higher than  $G''$ , which also demonstrated the emulsions were in typical pseudoplastic fluid states (Chen et al., 2012; Lin et al., 2024). Both the emulsions (Fig. 7A–C) and the gelatin solutions (Fig. 3F) showed

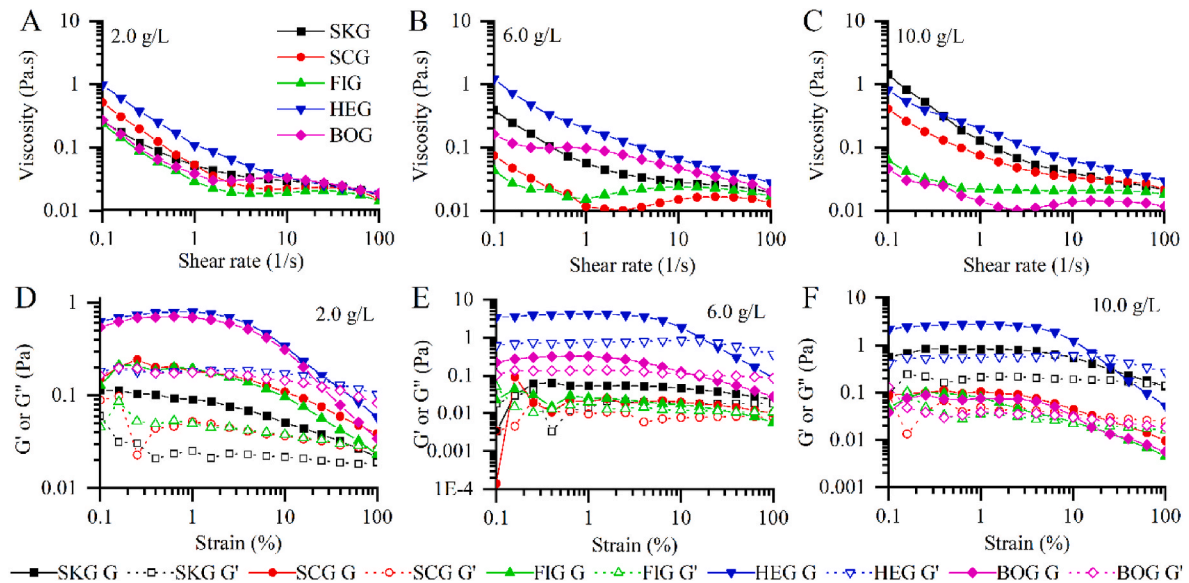


Fig. 7. Rheological properties of fish oil-loaded emulsions stabilized by silver carp by-product gelatins at different concentrations. (A–C): Viscosity vs. shear rate. (D–F):  $G'$  or  $G''$  vs. strain.

pseudoplastic fluid behaviors, which might result from that the emulsion droplets were stabilized by gelatins. Similar to the gelatin solutions (Fig. 3G), the emulsions also showed a gelatin source dependence of the  $G'$  and  $G''$  values.

#### 4. Conclusions

This work suggested that the structural properties of fish gelatins were dependent on the gelatin tissue sources (skin, scale, fin, head, and bone) and gelatin concentrations. The gel strength values of the gelatins in glass beakers were dependent on the gelatin tissue sources: skin  $\approx$  fin  $>$  scale  $>$  bone  $\approx$  head. Moreover, the gelatins were promising replacers as mammalian gelatin with high-Bloom (200–300 Bloom) for the commercial application in food industry. The rheological measurements suggested that scale and bone gelatin solutions had significantly lower apparent viscosities than other by-product gelatin solutions. The physicochemical properties were dependent on the molecular structures and nanoscale aggregate structures of the silver carp by-product gelatins. Further work is necessary to analyze the key factors to affect the physicochemical properties of gelatins.

These results suggested the emulsifying properties were also dependent on the molecular structures, nanoscale aggregate structures, and the physicochemical properties of the silver carp by-product gelatins. The interfacial tension and rheological apparent viscosity values of the emulsions were dependent on the gelatin tissue sources and gelatin concentrations. In particular, skin, scale, and fin gelatins induced no obvious emulsion creaming at the gelatin concentration of 10 g/L during the emulsion storage. Bone-related gelatins induced higher emulsion CI values for the emulsions with 10 g/L of gelatins during the emulsion storage. Therefore, these three gelatins might be promising emulsifiers for novel food development. Considering the used silver carp by-products were obtained from an aquatic factory, this work provided a promising way for the value-added utilization of aquatic by-products.

Further researches are necessary to develop and apply these gelatins from different tissue sources in the future. First, it is important to further analyze the physicochemical and functional properties such as the melting points, gelling points, Zeta potential, and foaming properties. Second, it is important to increase the production yields of gelatins from head (3.4%), fin (3.0%), and spine bone (1.4%) or scale up the production process to obtain sufficient gelatins for the potential application. Finally, it is interesting to develop novel foods with the gelatins from different tissue sources.

#### CRedit authorship contribution statement

**Guangyi Kan:** Investigation, Data curation, Formal analysis, Writing – original draft. **Li Li:** Investigation. **Huan Gong:** Investigation. **Lijia Chen:** Investigation. **Xichang Wang:** Supervision. **Jian Zhong:** Conceptualization, Data curation, Investigation, Funding acquisition, Supervision, Writing – review & editing.

#### Conflict of interest

The authors declare no conflict of interest.

#### Declaration of competing interest

The authors declare that they have no known competing financial interests or personal relationships that could have appeared to influence the work reported in this paper.

#### Acknowledgments

This research has been supported by research grants from the National Natural Science Foundation of China (No. 32272338) and the Shanghai Municipal Three-Year Action Plan for Strengthening the

Construction of Public Health System (2023–2025) Discipline Leader Project (GWVI-11.2-XD19).

#### Appendix A. Supplementary data

Supplementary data to this article can be found online at <https://doi.org/10.1016/j.crfs.2024.100894>.

#### Data availability

Data will be made available on request.

#### References

- Bai, Y., Luo, Q., Liu, J., 2016. Protein self-assembly via supramolecular strategies. *Chem. Soc. Rev.* 45, 2756–2767. <https://doi.org/10.1039/C6CS00004E>.
- Boran, G., Regenstein, J.M., 2009. Optimization of gelatin extraction from silver carp skin. *J. Food Sci.* 74, E432–E441. <https://doi.org/10.1111/j.1750-3841.2009.01328.x>.
- Chen, B., Li, H., Ding, Y., Suo, H., 2012. Formation and microstructural characterization of whey protein isolate/beet pectin coacervations by laccase catalyzed cross-linking. *LWT - Food Sci. Technol. (Lebensmittel-Wissenschaft -Technol.)* 47, 31–38. <https://doi.org/10.1016/j.lwt.2012.01.006>.
- Chen, J., Li, Y., Wang, Y., Yakubu, S., Tang, H., Li, L., 2022. Active polylactic acid/tilapia fish gelatin-sodium alginate bilayer films: application in preservation of Japanese sea bass (*Lateolabrax japonicus*). *Food Packag. Shelf Life* 33, 100915. <https://doi.org/10.1016/j.foodpack.2022.100915>.
- Chen, Y., Sun, Y., Ding, Y., Ding, Y., Liu, S., Zhou, X., Wu, H., Xiao, J., Lu, B., 2024. Recent progress in fish oil-based emulsions by various food-grade stabilizers: fabrication strategy, interfacial stability mechanism and potential application. *Crit. Rev. Food Sci. Nutr.* 64, 1677–1700. <https://doi.org/10.1080/10408398.2022.2118658>.
- Ding, M., Zhang, T., Zhang, H., Tao, N., Wang, X., Zhong, J., 2019. Effect of preparation factors and storage temperature on fish oil-loaded crosslinked gelatin nanoparticle pickering emulsions in liquid forms. *Food Hydrocolloids* 95, 326–335. <https://doi.org/10.1016/j.foodhyd.2019.04.052>.
- Ding, M., Zhang, T., Zhang, H., Tao, N., Wang, X., Zhong, J., 2020a. Gelatin-stabilized traditional emulsions: emulsion forms, droplets, and storage stability. *Food Sci. Hum. Wellness* 9, 320–327. <https://doi.org/10.1016/j.fshw.2020.04.007>.
- Ding, M., Zhang, T., Zhang, H., Tao, N., Wang, X., Zhong, J., 2020b. Gelatin molecular structures affect behaviors of fish oil-loaded traditional and Pickering emulsions. *Food Chem.* 309, 125642. <https://doi.org/10.1016/j.foodchem.2019.125642>.
- Du, Q., Zhou, L., Li, M., Lyu, F., Liu, J., Ding, Y., 2022. Omega-3 polyunsaturated fatty acid encapsulation system: physical and oxidative stability, and medical applications. *Food Front.* 3, 239–255. <https://doi.org/10.1002/fft2.134>.
- Feng, X., Fu, C., Yang, H., 2017. Gelatin addition improves the nutrient retention, texture and mass transfer of fish balls without altering their nanostructure during boiling. *LWT* 77, 142–151. <https://doi.org/10.1016/j.lwt.2016.11.024>.
- Gong, H., Kan, G., Li, L., Chen, L., Zi, Y., Shi, C., Wang, X., Zhong, J., 2024a. Effects of the extraction temperatures on the protein contents, gelatin purities, physicochemical properties, and functional properties of tilapia scale gelatins. *Int. J. Biol. Macromol.* 278, 135040. <https://doi.org/10.1016/j.ijbiomac.2024.135040>.
- Gong, H., Zi, Y., Kan, G., Li, L., Shi, C., Wang, X., Zhong, J., 2024b. Preparation of food-grade EDC/NHS-crosslinked gelatin nanoparticles and their application for Pickering emulsion stabilization. *Food Chem.* 436, 137700. <https://doi.org/10.1016/j.foodchem.2023.137700>.
- Hasanuddin, H., Jaziri, A.A., Shapawi, R., Mokhtar, R.A.M., Noordin, W.N.M., Huda, N., 2024. Effect of different acids during collagen extraction the bone and fins from purple-spotted bigeye (*Priacanthus tayenus* Richardson, 1846) and their physicochemical properties. *Food Res.* 8, 326–335. [https://doi.org/10.26656/fr.2017.8\(1\).224](https://doi.org/10.26656/fr.2017.8(1).224).
- Haug, L.J., Draget, K.I., 2011. 5 - gelatin. In: Phillips, G.O., Williams, P.A. (Eds.), *Handbook of Food Proteins*. Woodhead Publishing, Cambridge, UK, pp. 92–115.
- Huang, T., Tu, Z., Zou, Z., Shanguan, X., Wang, H., Bansal, N., 2020. Glycosylated fish gelatin emulsion: rheological, tribological properties and its application as model coffee creamers. *Food Hydrocolloids* 102, 105552. <https://doi.org/10.1016/j.foodhyd.2019.105552>.
- Jawdhari, A., Mihăilescu, D.F., Fendrihan, S., Jueva, V., Stoilov-Linu, V., Negrea, B.-M., 2022. Silver carp (*Hypophthalmichthys molitrix*) (asian silver carp) presence in Danube Delta and Romania—a review with data on natural reproduction. *Life* 12, 1582. <https://doi.org/10.3390/life12101582>.
- Kotodziejska, I., Skierka, E., Sadowska, M., Kotodziejski, W., Niecikowska, C., 2008. Effect of extracting time and temperature on yield of gelatin from different fish offal. *Food Chem.* 107, 700–706. <https://doi.org/10.1016/j.foodchem.2007.08.071>.
- Le, Y., Yang, H., 2022. Xanthan gum modified fish gelatin and binary culture modulates the metabolism of probiotics in fermented milk mainly via amino acid metabolism pathways. *Food Res. Int.* 161, 111844. <https://doi.org/10.1016/j.foodres.2022.111844>.
- Li, H., Van der Meer, P., 2022. Sequential adsorption of whey proteins and low methoxy pectin at the oil-water interface: an interfacial rheology study. *Food Hydrocolloids* 128, 107570. <https://doi.org/10.1016/j.foodhyd.2022.107570>.

- Lin, Q., Shang, M., Li, X., Sang, S., Chen, L., Long, J., Jiao, A., Ji, H., Qiu, C., Jin, Z., 2024. Rheology and 3D printing characteristics of heat-inducible pea protein-carrageenan-glycyrrhizic acid emulsions as edible inks. *Food Hydrocolloids* 147, 109347. <https://doi.org/10.1016/j.foodhyd.2023.109347>.
- Liu, J., Kong, X., Wang, C., Yang, X., 2023. Permeability of wood impregnated with polyethylene wax emulsion in vacuum. *Polymer* 281, 126123. <https://doi.org/10.1016/j.polymer.2023.126123>.
- Lv, L.-C., Huang, Q.-Y., Ding, W., Xiao, X.-H., Zhang, H.-Y., Xiong, L.-X., 2019. Fish gelatin: the novel potential applications. *J. Funct. Foods* 63, 103581. <https://doi.org/10.1016/j.jff.2019.103581>.
- Netter, A.B., Goudoulas, T.B., Germann, N., 2020. Effects of Bloom number on phase transition of gelatin determined by means of rheological characterization. *LWT* 132, 109813. <https://doi.org/10.1016/j.lwt.2020.109813>.
- Nie, Y., Chen, J., Xu, J., Zhang, Y., Yang, M., Yang, L., Wang, X., Zhong, J., 2022. Vacuum freeze-drying of tilapia skin affects the properties of skin and extracted gelatins. *Food Chem.* 374, 131784. <https://doi.org/10.1016/j.foodchem.2021.131784>.
- Noguchi, T., Sugiura, M., 2003. Analysis of flash-induced ftir difference spectra of the s-state cycle in the photosynthetic water-oxidizing complex by uniform <sup>15</sup>N and <sup>13</sup>C isotope labeling. *Biochemistry* 42, 6035–6042. <https://doi.org/10.1021/bi0341612>.
- Peng, J., Zi, Y., Xu, J., Zheng, Y., Huang, S., Hu, Y., Liu, B., Wang, X., Zhong, J., 2022. Effect of extraction methods on the properties of tilapia scale gelatins. *Int. J. Biol. Macromol.* 221, 1150–1160. <https://doi.org/10.1016/j.ijbiomac.2022.09.094>.
- Primoic, M., Duchek, A., Nickerson, M., Ghosh, S., 2017. Effect of lentil proteins isolate concentration on the formation, stability and rheological behavior of oil-in-water nanoemulsions. *Food Chem.* 237, 65–74. <https://doi.org/10.1016/j.foodchem.2017.05.079>.
- Ruan, Q., Chen, W., Lv, M., Zhang, R., Luo, X., Yu, E., Pan, C., Ma, H., 2023. Influences of trypsin pretreatment on the structures, composition, and functional characteristics of skin gelatin of tilapia, grass carp, and sea perch. *Mar. Drugs* 21, 423. <https://doi.org/10.3390/md21080423>.
- Shi, C., Bi, C., Ding, M., Xie, J., Xu, C., Qiao, R., Wang, X., Zhong, J., 2019. Polymorphism and stability of nanostructures of three types of collagens from bovine flexor tendon, rat tail, and tilapia skin. *Food Hydrocolloids* 93, 253–260. <https://doi.org/10.1016/j.foodhyd.2019.02.035>.
- Shyni, K., Hema, G.S., Ninan, G., Mathew, S., Joshy, C.G., Lakshmanan, P.T., 2014. Isolation and characterization of gelatin from the skins of skipjack tuna (*Katsuwonus pelamis*), dog shark (*Scoliodon sorrakowah*), and rohu (*Labeo rohita*). *Food Hydrocolloids* 39, 68–76. <https://doi.org/10.1016/j.foodhyd.2013.12.008>.
- Wang, Y., Tu, X., Shi, L., Yang, H., 2023. Quality characteristics of silver carp surimi gels as affected by okara. *Int. J. Food Prop.* 26, 49–64. <https://doi.org/10.1080/10942912.2022.2153863>.
- Wanyi, W., Lu, L., Zehan, H., Xinan, X., 2020. Comparison of emulsifying characteristics of different macromolecule emulsifiers and their effects on the physical properties of lycopene nanoemulsions. *J. Dispersion Sci. Technol.* 41, 618–627. <https://doi.org/10.1080/01932691.2019.1610421>.
- Wu, W., Xu, J., Yang, L., Yang, M., Zhang, T., Wang, X., Zhong, J., 2022. Self-assembled hydrolyzed gelatin nanoparticles from silver carp spine bones for Pickering emulsion stabilization. *Food Biosci.* 48, 101735. <https://doi.org/10.1016/j.fbio.2022.101735>.
- Xu, J., Zhang, T., Zhang, Y., Yang, L., Nie, Y., Tao, N., Wang, X., Zhong, J., 2021. Silver carp scale gelatins for the stabilization of fish oil-loaded emulsions. *Int. J. Biol. Macromol.* 186, 145–154. <https://doi.org/10.1016/j.ijbiomac.2021.07.043>.
- Yang, L., Yang, M., Xu, J., Nie, Y., Wu, W., Zhang, T., Wang, X., Zhong, J., 2022a. Structural and emulsion stabilization comparison of four gelatins from two freshwater and two marine fish skins. *Food Chem.* 371, 131129. <https://doi.org/10.1016/j.foodchem.2021.131129>.
- Yang, M., Yang, L., Xu, J., Nie, Y., Wu, W., Zhang, T., Wang, X., Zhong, J., 2022b. Comparison of silver carp fin gelatins extracted by three types of methods: molecular characteristics, structure, function, and pickering emulsion stabilization. *Food Chem.* 368, 130818. <https://doi.org/10.1016/j.foodchem.2021.130818>.
- Yu, D., Chi, C.-F., Wang, B., Ding, G.-F., Li, Z.-R., 2014. Characterization of acid-and pepsin-soluble collagens from spines and skulls of skipjack tuna (*Katsuwonus pelamis*). *Chin. J. Nat. Med.* 12, 712–720. [https://doi.org/10.1016/S1875-5364\(14\)60110-2](https://doi.org/10.1016/S1875-5364(14)60110-2).
- Yu, E., Pan, C., Luo, X., Ruan, Q., Chen, W., Fang, Y., Wang, K., Qin, Y., Lv, M., Ma, H., 2023. Structural characteristics, component interactions and functional properties of gelatins from three fish skins extracted by five methods. *Int. J. Biol. Macromol.* 248, 125813. <https://doi.org/10.1016/j.ijbiomac.2023.125813>.
- Zhang, H., Huang, X., Zhang, Y., Zou, X., Tian, L., Hong, H., Luo, Y., Tan, Y., 2023. Silver carp (*Hypophthalmichthys molitrix*) by-product hydrolysates: a new nitrogen source for *Bifidobacterium animalis ssp. lactis* BB-12. *Food Chem.* 404, 134630. <https://doi.org/10.1016/j.foodchem.2022.134630>.
- Zhang, L., Li, Q., Hong, H., Luo, Y., 2020. Prevention of protein oxidation and enhancement of gel properties of silver carp (*Hypophthalmichthys molitrix*) surimi by addition of protein hydrolysates derived from surimi processing by-products. *Food Chem.* 316, 126343. <https://doi.org/10.1016/j.foodchem.2020.126343>.
- Zhang, T., Sun, R., Ding, M., Li, L., Tao, N., Wang, X., Zhong, J., 2020. Commercial cold-water fish skin gelatin and bovine bone gelatin: structural, functional, and emulsion stability differences. *LWT - Food Sci. Technol. (Lebensmittel-Wissenschaft -Technol.)* 125, 109207. <https://doi.org/10.1016/j.lwt.2020.109207>.
- Zhang, T., Xu, J., Huang, S., Tao, N., Wang, X., Zhong, J., 2022. Anhydride structures affect the acylation modification and emulsion stabilization ability of mammalian and fish gelatins. *Food Chem.* 375, 131882. <https://doi.org/10.1016/j.foodchem.2021.131882>.
- Zhang, T., Xu, J., Zhang, Y., Wang, X., Lorenzo, J.M., Zhong, J., 2020. Gelatins as emulsifiers for oil-in-water emulsions: extraction, chemical composition, molecular structure, and molecular modification. *Trends Food Sci. Technol.* 106, 113–131. <https://doi.org/10.1016/j.tifs.2020.10.005>.